

Calculations of electron scattering on H-like ions

I. Bray , H. Hayat, D. V. Fursa , and A. S. Kadyrov 

*Curtin Institute for Computation and Department of Physics and Astronomy, Curtin University,
GPO Box U1987, Perth, WA 6845, Australia*

A. W. Bray 

Research School of Physics and Engineering, The Australian National University, Canberra ACT 0200, Australia

M. Cytowski 

Pawsey Supercomputing Centre, 1 Bryce Ave., Kensington, WA 6151, Australia



(Received 21 October 2019; accepted 9 January 2020; published 10 February 2020)

Electron-impact excitation and ionization of H-like ions of nuclear charge $Z = 2, \dots, 8$ have been calculated from thresholds to high energies, with a particular focus on spin asymmetry of the cross sections. It is found that the importance of electron exchange is undiminished with increasing Z . Away from resonance regions, scaling considerations allow for accurate nonrelativistic estimates of the total-electron-spin-dependent cross sections for $Z > 8$.

DOI: [10.1103/PhysRevA.101.022703](https://doi.org/10.1103/PhysRevA.101.022703)

I. INTRODUCTION

The field of electron-ion scattering has considerable history and utility. Several reviews are available on the subject; see, for example, Müller [1], Williams [2], and Bartschat and Kushner [3]. Presently, our interest is in the simplest one-electron ionic targets and particularly in the electron-spin-dependent cross sections. Any nonzero electron-spin target has two independent total-electron-spin S components. Experiments that are able to resolve electron-spin phenomena are relatively rare. However, they are invaluable in the testing of theory; see the review of Andersen *et al.* [4] for extensive examples. Furthermore, the behavior of the cross sections for different S can be remarkably different [5].

Electron collisions with H-like ions are Coulomb three-body problems. These are generally regarded as solved problems utilizing modern computational techniques whose validity is independent of the projectile energy. Such methods include R matrix with pseudostates [6–8], time-dependent close coupling [9], and convergent close coupling [10]. The current focus of the field has moved to more complicated collision systems, as discussed by Schippers *et al.* [11]. However, there is still some interesting physics to be found, and also, there is a requirement for complete data sets for practical applications.

Recently, Bray *et al.* [12] found that with increasing charge q of He-like ions, in the initial metastable 2^3S state, the ionization spin asymmetries converged rapidly to a constant as a function of $u = E_i/E_I$, where E_i is the incident electron energy and E_I is the ionization threshold. Examination of the ionization spin asymmetries in electron scattering on Li-like targets in the ground state [13,14] also resulted in the same conclusion [12]. The consequence of this is that the importance of electron exchange remains undiminished with increasing q , even though the incident energies increase as q^2 . Furthermore, the spin asymmetries exhibited uniform

behavior where the cross section for one of the two total electron spins dominated the other.

Here we check these ideas for H-like ions in the ground state, not only for ionization, but for excitation cross sections as well. In the process we generate complete data sets that allow for self-consistent applications in collisional-radiative models [15].

II. CONVERGENT CLOSE-COUPPLING THEORY

The convergent close-coupling theory (CCC) theory was initially developed for e -H scattering [16] and then extended to H-like targets [17]. Presently, it has been extended to atomic and molecular targets that can be modeled as quasi one- or two-electron targets. In addition, projectiles now include photons, positrons and bare ions. For light projectiles the method is valid for all projectile energies, and with the analytical treatment of the singularity in the Green's function [18], this includes zero final energies (excitation thresholds). CCC is based on solving coupled Lippmann-Schwinger equations in momentum space upon expansion of the total wave function in a Laguerre basis. Some of the more recent reviews of applications of the CCC theory to diverse collision systems are given in Refs. [19–22].

We are interested in calculating electron scattering on H-like ions and begin by determining the parameters of the Laguerre basis,

$$\xi_{kl}(r) = \sqrt{\frac{\lambda_l(k-1)!}{(2l+1+k)!}} (\lambda_l r)^{l+1} \exp(-\lambda_l r/2) L_{k-1}^{2l+2}(\lambda_l r), \quad (1)$$

where $L_{k-1}^{2l+2}(\lambda_l r)$ are the associated Laguerre polynomials. Possible values of k range from 1 to the basis size N_l , and $0 \leq l \leq l_{\max}$. As usual, we set $N_l = N_0 - l$ and $\lambda_l = \lambda$. Presently,

we take $l_{\max} = 3$, $N_0 = 25$, and $\lambda = Z$, where Z is the nuclear charge of the ion. The target states ϕ_n , $n = 1, \dots, N_l$ are linear combinations of the Laguerre basis functions and satisfy

$$\langle \phi_f | H_T | \phi_i \rangle = \epsilon_f \delta_{fi}, \quad (2)$$

where H_T is the target Hamiltonian. With such a choice we obtain discrete ionic eigenstates of principal quantum number $n \leq 7$ and a sufficiently dense discretization of the continuum, which renders any pseudoresonances to be insignificant.

The calculations are performed on a broad range of energies, from excitation thresholds to around 10 times the ionization threshold. The excitation and ionization thresholds, in electronvolts, are

$$E_n = (1 - n^{-2})Z^2 \text{Ry} \quad \text{and} \quad E_I = Z^2 \text{Ry}, \quad (3)$$

respectively, where $\text{Ry} = 13.6057 \text{ eV}$ is the Rydberg constant. We use a fine energy mesh below the ionization threshold to ensure major resonances are found and a more coarse energy mesh above the ionization threshold.

For a given incident electron energy, integrated cross sections $\sigma_f(S)$ are generated for all open final target states of $\epsilon_f < E_i + \epsilon_i$, where ϵ_i is the energy of the initial target state and $S = 0, 1$ is the total electron spin. The spin-averaged cross section σ_f and the corresponding spin asymmetry A_f are

$$\sigma_f = \frac{\sigma_f(0) + 3\sigma_f(1)}{4} \quad \text{and} \quad A_f = \frac{\sigma_f(0) - \sigma_f(1)}{\sigma_f(0) + 3\sigma_f(1)}. \quad (4)$$

In the CCC method the total ionization cross section is obtained by summing the cross sections for all target states ϕ_f for which $\epsilon_f > 0$. The spin asymmetry parameter ranges from $A_f = -1/3$, whenever $\sigma_f(1) \gg \sigma_f(0)$, to $A_f = 1$, whenever $\sigma_f(0) \gg \sigma_f(1)$. A value of zero indicates that electron exchange is negligible, and this is the limit with increasing incident energy.

As we are interested in ionic targets with asymptotic charge $q = Z - 1 \geq 1$, we need to generalize Eq. (8) of Bray *et al.* [18] for the case of zero energy, as happens at the excitation thresholds. The regular and irregular Coulomb functions for q of interest, in the limit of zero energy, can be obtained from

$$\begin{aligned} \lim_{k_n \rightarrow 0} f_L(k_n r, q) / \sqrt{k_n} &= \sqrt{\pi r} J_{2L+1}(\sqrt{8qr}), \\ \lim_{k_n \rightarrow 0} g_L(k_n r, q) / \sqrt{k_n} &= -\sqrt{\pi r} Y_{2L+1}(\sqrt{8qr}), \end{aligned} \quad (5)$$

where J and Y are the cylindrical Bessel functions of the first and second kind, respectively.

The CCC computer code for electron scattering has recently completed its third generation of parallel processing implementation. It is now able to utilize graphics processing units (GPUs) in addition to OpenMP (multicore) and MPI (multinode) implementation. The details will be discussed elsewhere, but we note that the GPU implementation leads to 1–2 orders of magnitude speedup. We take advantage of this for the first time in this work, which required many energies, partial waves, and targets.

III. RESULTS

We begin by validating the CCC calculations for the total ionization cross sections, where experimental data are

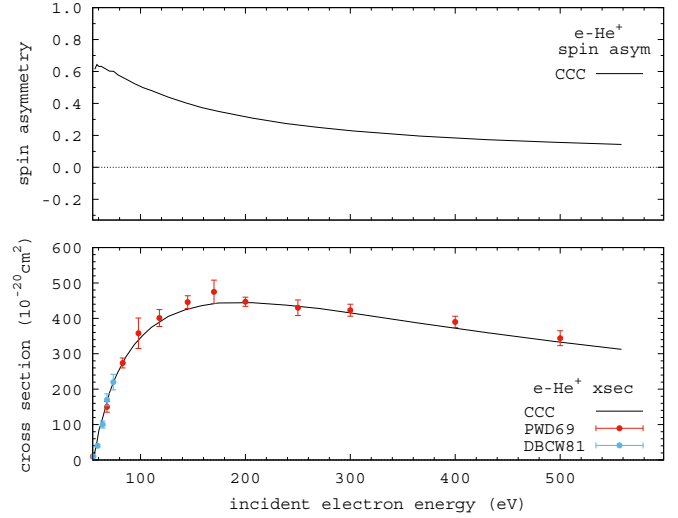


FIG. 1. Cross section (bottom) and its spin asymmetry (top) for electron-impact total ionization of He^+ . The CCC calculations are described in the text. The experimental data are due to Peart *et al.* [23] and Defrance *et al.* [24].

available. In doing so we also establish the required incident electron energies E_i for each target.

A. Ionization

In Figs. 1–6 the electron-impact total ionization cross section and its spin asymmetry are presented for the specified ions. We see excellent agreement with experiment for the cross sections. The spin asymmetries all have the same shape, starting at a positive value at the corresponding threshold and diminishing monotonically towards zero with increasing energy. The fact that they remain above zero at all energies is due to the fact that the direct and exchange contributions are combined with the factor of $(-1)^S$ for singlet ($S = 0$) and triplet ($S = 1$) scattering. This explanation assumes that the

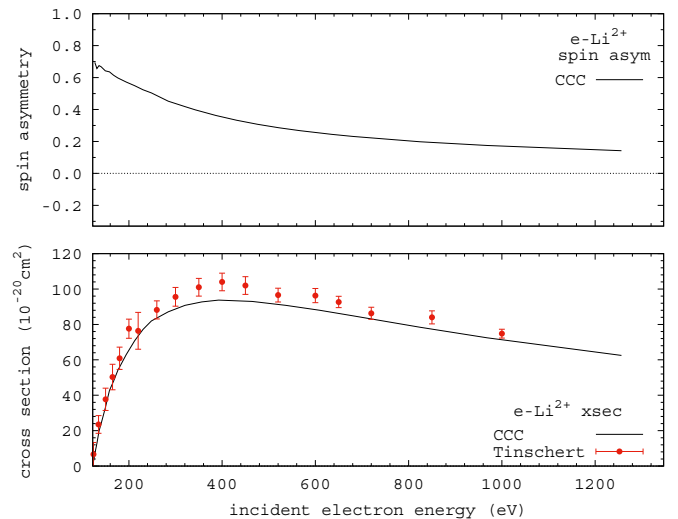


FIG. 2. As for Fig. 1, except for the Li^{2+} target with the experimental data due to Tinschert *et al.* [25].

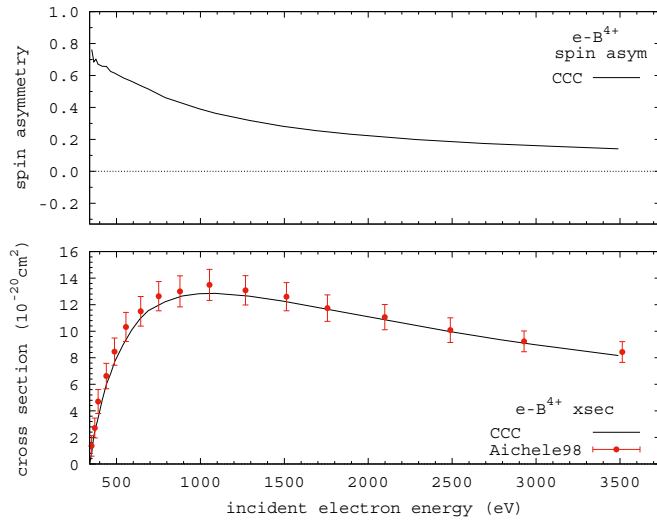


FIG. 3. As for Fig. 1, except for the B^{4+} target with the experimental data due to Aichele *et al.* [27].

direct and exchange components are of a similar sign. We shall see later that this is not always the case.

Note that in the case of ionization we cannot obtain accurate results too close to the threshold. This is because of limitations in practical discretization of the target continuum via the Laguerre basis. Accurate results for ionization are only possible once the number of open positive-energy states is sufficiently large. Nevertheless, we see that the CCC method is able to get quite close to the threshold here, as has been demonstrated previously when addressing near-threshold behavior of ionization [26].

Having found good agreement of the calculated total ionization cross sections with experiment, we now turn to scaling considerations as proposed by Burgess and Rudge [28], Burgess *et al.* [29], and Younger [30]. In Fig. 7 the cross sections presented above have been multiplied by their corresponding E_1^2 (in effect Z^4) and plotted as a function of $u = E_i/E_1$.

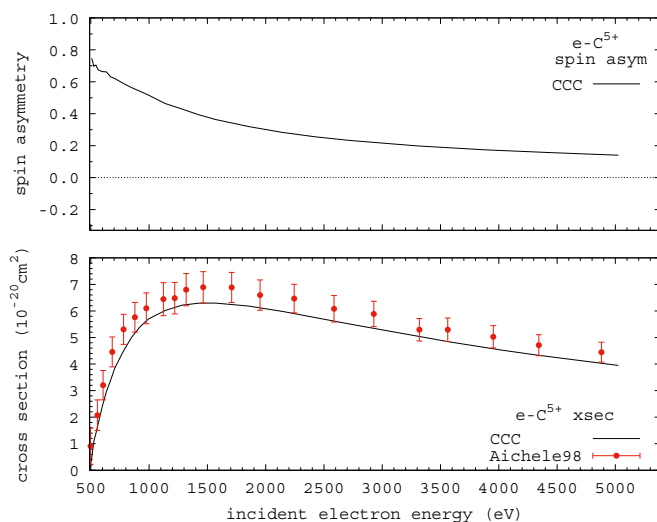


FIG. 4. As for Fig. 3, except for the C^{5+} target.

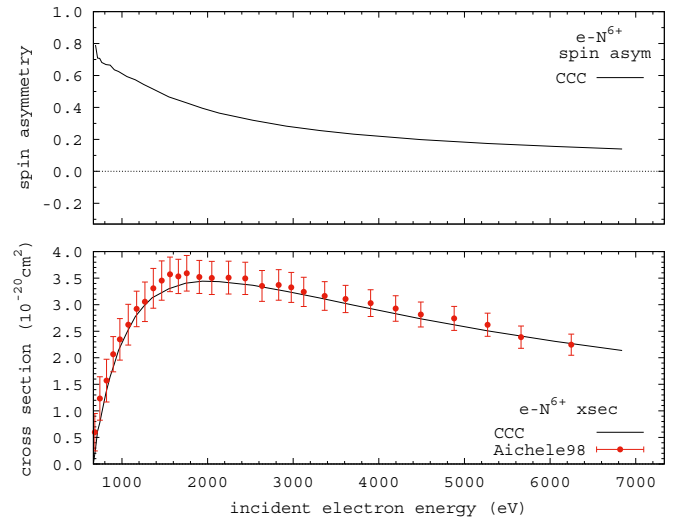


FIG. 5. As for Fig. 3, except for the N^{6+} target.

Starting with the scaled cross sections, we see that they systematically increase and converge with increasing Z , allowing for an accurate estimate of cross sections for $Z > 8$. The spin asymmetries also increase systematically, and converge even more rapidly than the scaled cross sections, with increasing Z . Thus, despite requiring larger energies with increasing Z , electron exchange remains significant at the considered energies, which can be as high as 9 keV for the O^{7+} ion. In light of similar findings for other targets [12] these results are not surprising, though they needed to be confirmed. We next consider discrete excitation.

B. Excitation

Due to unitarity of the CCC formalism, reliability of the CCC calculations for ionization cross sections indicates reliability of the corresponding discrete excitation cross sections as well. In obtaining complete data sets for electron-ion scattering, to be utilized in collisional-radiative models, it is helpful to have excitation cross sections begin at exactly their thresholds. As an example, here we start at the $n = 2$

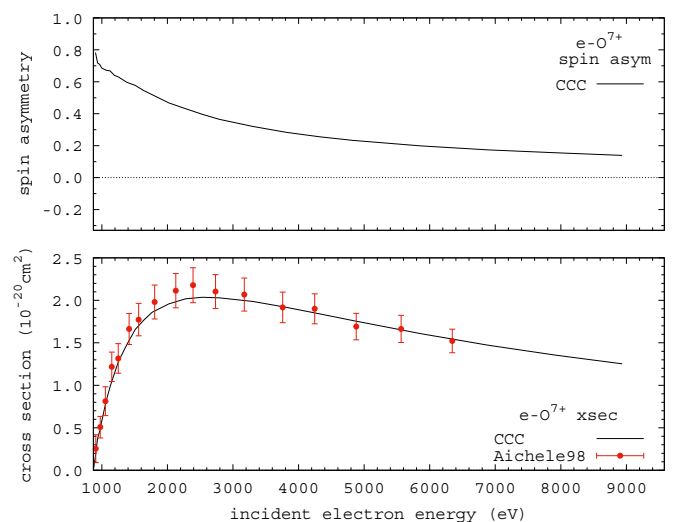


FIG. 6. As for Fig. 3, except for the O^{7+} target.

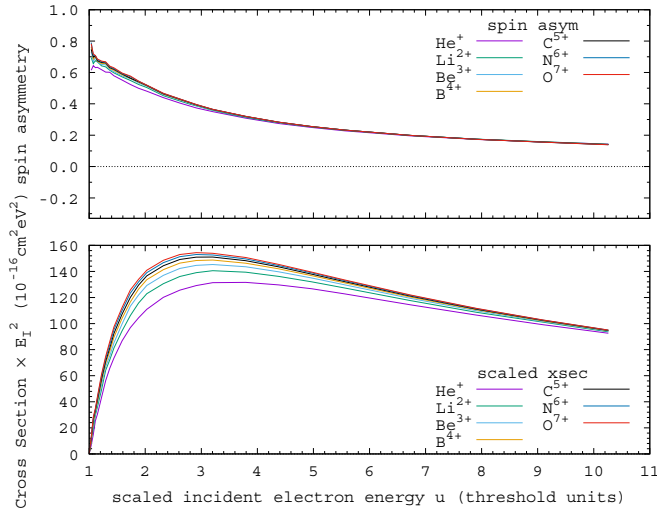


FIG. 7. Spin asymmetries and scaled, by E_1^2 , cross sections of Figs. 1–6 as a function of $u = E_i/E_1$.

thresholds, see Eq. (3). Rather than showing cross sections for individual targets separately, as we did for ionization, we combine them together to immediately focus on the scaling considerations.

In Fig. 8 the spin asymmetries and scaled cross sections are given for all considered ions as a function of $u = E_i/E_{n=2}$, where $E_{n=2}$ is the energy of the $n = 2$ threshold. We use a logarithmic scale for u in order to emphasize the lower energy region, to show the values at the exact threshold, and to broaden the resonance region. We see that away from this region the scaling behavior is much the same as for the ionization case. Here spin asymmetries converge even more rapidly than the cross sections. Convergence is systematic and monotonic, with the singlet cross sections being dominant over the triplet ones over the entire energy range. The results for $2P$ excitation are given in Fig. 9, and the same conclusions as for $2S$ excitation apply.

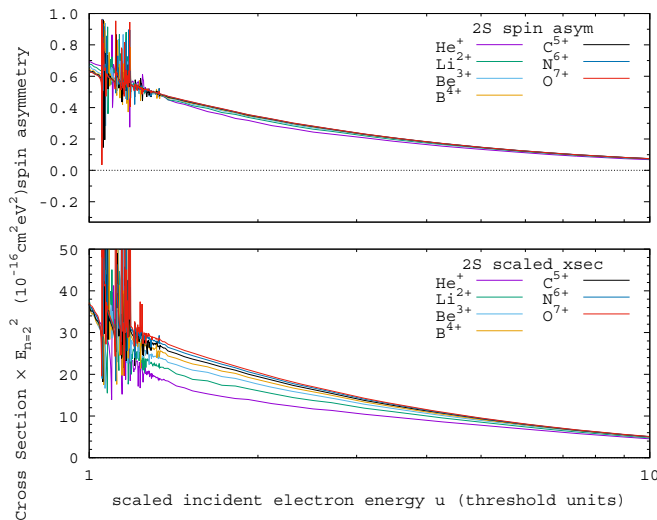


FIG. 8. Spin asymmetries and scaled, by $E_{n=2}^2$, cross sections for electron-impact $2S$ excitation of H-like ions as a function of $u = E_i/E_{n=2}$.

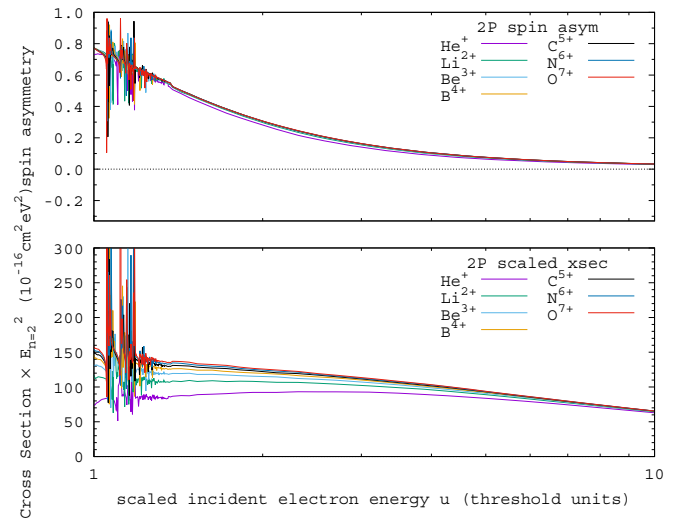


FIG. 9. Spin asymmetries and scaled, by $E_{n=2}^2$, cross sections for electron-impact $2P$ excitation of H-like ions as a function of $u = E_i/E_{n=2}$.

C. Elastic scattering

We next consider elastic scattering. Note that we present only the results arising from the close-coupling part of the CCC calculations. Due to the additional contribution of Rutherford scattering the physical elastic electron-ion cross sections are infinite. Nevertheless, accurate matrix elements for elastic transitions have application in the analysis of Stark broadening [31,32] and also help to check the unitarity of the close-coupling calculations. The elastic scattering case is different from the others considered as it has no threshold, and so for scaling purposes we use Z instead.

In Fig. 10 we present the elastic scattering spin asymmetries and scaled, by Z^4 , cross sections against $u = E_i/Z^2$. For consistency and ease of comparison the energy range is the same as used for excitation, i.e., above the $E_{n=2}$ threshold. We see that the Z^4 scaled elastic scattering cross sections appear

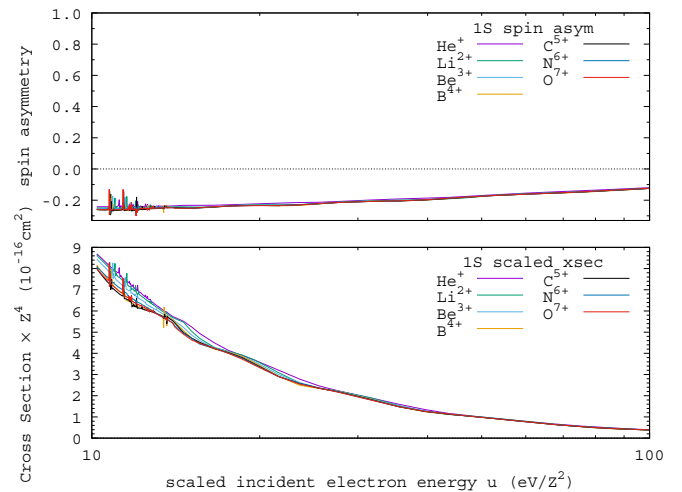


FIG. 10. Spin asymmetries and scaled, by Z^4 , cross sections for elastic scattering of electrons on the ground state of H-like ions as a function of $u = E_i/Z^2$. Note that the Rutherford term has not been included.

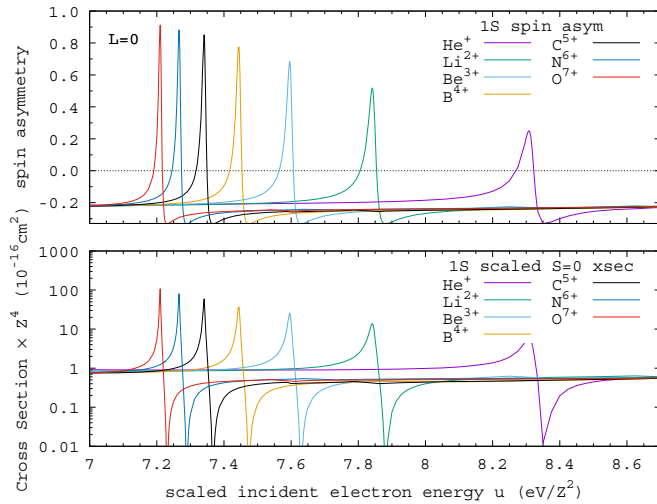


FIG. 11. Zeroth partial-wave spin asymmetries and scaled, by Z^4 , singlet cross sections for elastic scattering of electrons on the ground state of H-like ions as a function of $u = E_i/Z^2$.

to converge even faster than those for $2S$ and $2P$ excitation. What is more interesting is that the spin asymmetry, which is almost identical for all targets considered as a function of u , has a completely different behavior to that previously seen. Now we find it to be negative, indicating that triplet scattering is dominant, or equivalently, direct and exchange contributions have the opposite sign for elastic scattering. The origin of this difference is that only in the elastic channel does the direct potential have the $-1/r$ term occurring [see Eq. (52) of Bray and Stelbovics [10]]. It comes from the nuclear potential $-Z/r$, with the Coulomb waves calculated for $q = Z - 1$, leaving only $-1/r$ in the direct matrix element calculation. This is sufficient to change the sign of the radial potentials when calculating the direct matrix elements.

Lastly, to elucidate the scaling behavior of resonances, we take the example of the resonance below the $E_{n=2}$ threshold in the singlet elastic zeroth partial wave, corresponding to the formation of the two-electron $(2s^2)^1S$ autoionizing He-like state. These results are presented in Fig. 11 using the same scaling as in Fig. 10. We see that the resonances systematically shift towards the lower values of u and also become narrower, growing rapidly with increasing Z . Thus they do not scale as simply as the underlying cross sections. This is not surprising, since the scaling proposed by Burgess *et al.* [29] relates just to the target properties whose energies have the Z^2 factor given in Eq. (3). The resonances are due to the combined electron-ion system. For all targets the triplet cross section $\sigma_{1s}(1)$ is smooth over the entire presented energy range, and so the spin asymmetries indicate the existence of Fano-type

resonances, with the singlet cross section varying rapidly from $\sigma_{1s}(0) \gg \sigma_{1s}(1)$ to $\sigma_{1s}(0) \ll \sigma_{1s}(1)$ over a very small energy range.

We have also analyzed the resonance structure in the excitation channels with the same conclusions as for the presented elastic-scattering case. Namely, with increasing Z the corresponding resonances move to lower energies u and become narrower but greater in magnitude. Hence, they cannot be readily estimated for higher Z using the scaling considered here. An overview of the resonances in discrete excitation has been given by Ballance *et al.* [6].

IV. CONCLUSIONS

Using the GPU-enabled CCC code, detailed and extensive calculations of electron scattering on H-like ions for $Z = 2, \dots, 8$ have been performed, from thresholds through to high energies. We confirmed the Z^4 scaling rule for the cross sections, and this may be generally used to obtain nonrelativistic spin-dependent cross sections for $Z > 8$. One exception is the resonance region below the ionization threshold, where the resonances change shape and move systematically to lower values as a function of the reduced energy $u = E_i/Z^2$. As found previously for He-like ions in the metastable initial state 2^3S and Li-like ions in the ground state [12], the spin asymmetries converge even more rapidly than the cross sections for a given value of u , indicating that exchange effects do not diminish with increasing Z . Generally, the spin asymmetries are dominated by the singlet case, with the exception of elastic scattering, where the triplet cross sections dominate. The complete data set for each $Z \leq 8$ has excitation cross sections for $n \leq 7$ and may be used in collisional-radiative models as a single self-consistent set with uncertainties, with uncertainties of the order of 5% away from resonance regions. For higher Z the existing data may be used to infer total ionization cross sections quite accurately until relativistic effects become important. This can be quantified using the Dirac-based fully relativistic CCC method [33–35].

ACKNOWLEDGMENTS

We thank Shiv Meka of Curtin University and John Stone of University of Illinois at Urbana-Champaign for their guidance in the GPU implementation. We acknowledge the Australian Research Council, and the resources and services of the National Computational Infrastructure and the Pawsey Supercomputer Centre, which are supported by the Australian and Western Australian Governments. This work also used the Extreme Science and Engineering Discovery Environment (XSEDE), which is supported by National Science Foundation Grant No. ACI-1548562.

- [1] A. Müller, *Electron Ion Collisions: Fundamental Processes in the Focus of Applied Research*, edited by E. Arimondo, P. R. Berman, and C. C. Lin, *Advances In Atomic, Molecular, and Optical Physics* Vol. 55 (Academic Press, New York, 2008), p. 293.
- [2] I. D. Williams, Electron-ion scattering, *Rep. Prog. Phys.* **62**, 1431 (1999).

- [3] K. Bartschat and M. J. Kushner, Electron collisions with atoms, ions, molecules, and surfaces: Fundamental science empowering advances in technology, *Proc. Natl. Acad. Sci. USA* **113**, 7026 (2016).
- [4] N. Andersen, K. Bartschat, J. T. Broad, and I. V. Hertel, Collisional alignment and orientation of atomic outer shells, III. Spin-resolved excitation, *Phys. Rep.* **279**, 251 (1997).

- [5] I. Bray, Close-Coupling Theory of Ionization: Successes and Failures, *Phys. Rev. Lett.* **78**, 4721 (1997).
- [6] C. P. Ballance, N. R. Badnell, and E. S. Smyth, A pseudo-state sensitivity study on hydrogenic ions, *J. Phys. B: At., Mol. Opt. Phys.* **36**, 3707 (2003).
- [7] K. Bartschat, The R-matrix with pseudo-states method: Theory and applications to electron scattering and photoionization, *Comput. Phys. Commun.* **114**, 168 (1998).
- [8] O. Zatsarinny, BSR: B-spline atomic R-matrix codes, *Comput. Phys. Commun.* **174**, 273 (2006).
- [9] M. S. Pindzola, F. Robicheaux, S. D. Loch, J. C. Berengut, T. Topcu, J. Colgan, M. Foster, D. C. Griffin, C. P. Ballance, D. R. Schultz, T. Minami, N. R. Badnell, M. C. Witthoef, D. R. Plante, D. M. Mitnik, J. A. Ludlow, and U. Kleiman, The time-dependent close-coupling method for atomic and molecular collision processes, *J. Phys. B: At., Mol. Opt. Phys.* **40**, R39 (2007).
- [10] I. Bray and A. T. Stelbovics, *Calculation of Electron Scattering on Hydrogenic Targets* (Academic Press, New York, 1995), p. 209.
- [11] S. Schippers, E. Sokell, F. Aumayr, H. Sadeghpour, K. Ueda, I. Bray, K. Bartschat, A. Murray, J. Tennyson, A. Dorn, M. Yamazaki, M. Takahashi, N. Mason, O. Novotný, A. Wolf, L. Sanche, M. Centurion, Y. Yamazaki, G. Laricchia, C. M. Surko *et al.*, Roadmap on photonic, electronic and atomic collision physics: II. Electron and antimatter interactions, *J. Phys. B: At., Mol. Opt. Phys.* **52**, 171002 (2019).
- [12] I. Bray, D. V. Fursa, A. S. Kadyrov, A. Müller, A. Borovik, and S. Schippers, Spin asymmetry in electron-impact ionization, *Phys. Rev. A* **100**, 012707 (2019).
- [13] I. Bray, Calculation of electron-impact ionization of lithium-like targets, *J. Phys. B: At., Mol. Opt. Phys.* **28**, L247 (1995).
- [14] K. Bartschat and I. Bray, Calculation of electron impact excitation and ionization of Be^+ , *J. Phys. B: At., Mol. Opt. Phys.* **30**, L109 (1997).
- [15] *Modern Methods in Collisional-Radiative Modeling of Plasmas*, edited by Y. Ralchenko, Springer Series on Atomic, Optical, and Plasma Physics Vol. 90 (Springer, New York, 2016).
- [16] I. Bray and A. T. Stelbovics, Convergent close-coupling calculations of electron-hydrogen scattering, *Phys. Rev. A* **46**, 6995 (1992).
- [17] I. Bray, Convergent close-coupling method for the calculation of electron scattering on hydrogen-like targets, *Phys. Rev. A* **49**, 1066 (1994).
- [18] A. Bray, I. Abdurakhmanov, A. Kadyrov, D. Fursa, and I. Bray, Solving close-coupling equations in momentum space without singularities for charged targets, *Comput. Phys. Commun.* **212**, 55 (2017).
- [19] I. Bray, D. V. Fursa, A. S. Kheifets, and A. T. Stelbovics, Electrons and photons colliding with atoms: Development and application of the convergent close-coupling method, *J. Phys. B: At., Mol. Opt. Phys.* **35**, R117 (2002).
- [20] A. S. Kadyrov and I. Bray, Recent progress in the description of positron scattering from atoms using the convergent close-coupling theory, *J. Phys. B: At., Mol. Opt. Phys.* **49**, 222002 (2016).
- [21] M. C. Zammit, D. V. Fursa, J. S. Savage, and I. Bray, Electron- and positron-molecule scattering: Development of the molecular convergent close-coupling method, *J. Phys. B: At., Mol. Opt. Phys.* **50**, 123001 (2017).
- [22] I. Bray, I. B. Abdurakhmanov, J. J. Bailey, A. W. Bray, D. V. Fursa, A. S. Kadyrov, C. M. Rawlins, J. S. Savage, A. T. Stelbovics, and M. C. Zammit, Convergent close-coupling approach to light and heavy projectile scattering on atomic and molecular hydrogen, *J. Phys. B: At., Mol. Opt. Phys.* **50**, 202001 (2017).
- [23] B. Peart, D. S. Walton, and K. T. Dolder, The ranges of validity of the Born and Bethe approximations for the single ionization of He^+ and Li^+ ions by electron impact, *J. Phys. B: At., Mol. Opt. Phys.* **2**, 1347 (1969).
- [24] P. Defrance, F. Brouillard, W. Claeys, and G. V. Wassenhove, Crossed beam measurement of absolute cross sections: An alternative method and its application to the electron impact ionisation of He^+ , *J. Phys. B* **14**, 103 (1981).
- [25] K. Tinschert, A. Müller, G. Hofmann, K. Huber, R. Becker, D. C. Gregory, and E. Salzborn, Experimental cross sections for electron impact ionisation of hydrogen-like Li^{2+} ions, *J. Phys. B: At., Mol. Opt. Phys.* **22**, 531 (1989).
- [26] I. Bray, A. W. Bray, D. V. Fursa, and A. S. Kadyrov, Near-Threshold Cross Sections for Electron and Positron Impact Ionization of Atomic Hydrogen, *Phys. Rev. Lett.* **121**, 203401 (2018).
- [27] K. Aichele, U. Hartenfeller, D. Hathiramani, G. Hofmann, V. Schäfer, M. Steidl, M. Stenke, E. Salzborn, T. Pattard, and J. M. Rost, Electron impact ionization of the hydrogen-like ions B^{4+} , C^{5+} , N^{6+} and O^{7+} , *J. Phys. B: At., Mol. Opt. Phys.* **31**, 2369 (1998).
- [28] A. Burgess and M. R. H. Rudge, The ionization of hydrogenic positive ions by electron impact, *Proc. R. Soc. London, Ser. A* **273**, 372 (1963).
- [29] A. Burgess, D. G. Hummer, and J. A. Tully, Electron impact excitation of positive ions, *Philos. Trans. R. Soc. London, Ser. A* **266**, 225 (1970).
- [30] S. M. Younger, Electron-impact ionization cross sections for highly ionized hydrogen- and lithium-like atoms, *Phys. Rev. A* **22**, 111 (1980).
- [31] Y. V. Ralchenko, H. R. Griem, I. Bray, and D. V. Fursa, Quantum-mechanical calculation of stark widths of Ne VII $n = 3$, $\Delta n = 0$ transitions, *Phys. Rev. A* **59**, 1890 (1999).
- [32] T. A. Gomez, T. Nagayama, C. J. Fontes, D. P. Kilcrease, S. B. Hansen, M. C. Zammit, D. V. Fursa, A. S. Kadyrov, and I. Bray, Effect of Electron Capture on Spectral Line Broadening in Hot Dense Plasmas, *Phys. Rev. Lett.* **124**, 055003 (2020).
- [33] D. V. Fursa and I. Bray, Fully Relativistic Convergent Close-Coupling Method for Excitation and Ionization Processes in Electron Collisions with Atoms and Ions, *Phys. Rev. Lett.* **100**, 113201 (2008).
- [34] C. J. Bostock, D. V. Fursa, and I. Bray, Relativistic convergent close-coupling method: Calculation of electron scattering from hydrogenlike ions, *Phys. Rev. A* **80**, 052708 (2009).
- [35] D. V. Fursa, C. J. Bostock, I. Bray, and C. J. Fontes, Calculations of electron-impact ionisation of Fe^{25+} and Fe^{24+} , *J. Phys. B: At., Mol. Opt. Phys.* **49**, 184001 (2016).